Materials Letters 363 (2024) 136252

Contents lists available at ScienceDirect

Materials Letters

journal homepage: www.elsevier.com/locate/matlet

# Exploring potential of MXenes in smart sensing and energy harvesting

J.A. Ajani Lakmini Jayarathna [a,c], Sugato Hajra [b], Swati Panda [b], Elham Chamanehpour [c], Indra Sulania [d], Manjeet Singh Goyat [c,e], Shu-Han Hsu [a], Hoe Joon Kim [b], Tanyakarn Treeratanaphitak [a], Yogendra Kumar Mishra [c,*]

[a] School of Integrated Science and Innovation, Sirindhorn International Institute of Technology (SIIT), Thammasat University, Pathum Thani 12120, Thailand
[b] Department of Robotics and Mechatronics Engineering, Daegu Gyeongbuk Institute of Science and Technology, Daegu 42988, South Korea
[c] Mads Clausen Institute, NanoSYD, University of Southern Denmark (SDU), Denmark
[d] Inter University Accelerator Centre, Materials Science Group, New Delhi, India
[e] Department of Applied Science, School of Engineering, University of Petroleum and Energy Studies, Dehradun 248007, India

ARTICLE INFO

*Keywords:*
MXene layer
Sensor
Piezo-resistive
Triboelectric

ABSTRACT

In present work, MXene based piezo-resistive stress sensor device is fabricated using a freeze-dry method. The device was tested to measure the mechanical stress, sensitivity, and triboelectric response by converting them into electrical signals as readout. With high electrical conductivity, mechanical flexibility, and piezo-resistive characteristics, MXene-based device offers novel sensing and triboelectric-related applications. This study showed an extensive characterization after fabricating the sensor using a simple and scalable process to ensure their performance in terms of sensitivity, stability, and repeatability. Using pure MXene layer as the core material, this paper pioneers an interesting investigation focusing on stress monitoring by piezoresistive stress sensor and triboelectric nanogenerator.

## 1. Introduction

Recently, the demand for innovative sensor materials is surging, driven by factors like cost-effectiveness, eco-friendliness, and mechanical robustness. MXene, a piezo-resistive material, is gaining prominence due to its exceptional electrical and mechanical properties rooted in its layered structure [1–3]. With a sensitivity of 148.26 $kPa^{-1}$ under pressure of up to 16 kPa, MXene is assumed to revolutionize next-gen biosensors, detecting human motion with varying pressures [4,5]. Ma et al., demonstrated a three-layered MXene-based sensing device with a remarkable gauge factor of ~ 180.1 $kPa^{-1}$ under loading/unloading pressures of up to 13 kPa [6]. Guo et al., explored that MXene-impregnated tissue paper showcases gauge factors of 0.55, 3.81, and 2.52 $kPa^{-1}$ for different pressure ranges [7].

Additionally, MXene is very promising for triboelectric nanogenerators (TENGs) and self-powered technologies [8]. TENG is an energy-harvesting device, which converts mechanical energy into electrical energy. Y Gao et al., demonstrated the importance of MXene for TENG and its electrical properties [9]. Additionally, MXene can be used to improve the performance of TENG [10]. Zhao et al., have demonstrated that MXene-based hybrid capacitor integrated system exhibits excellent areal capacity and cycling stability [11]. Li *et al.,* constructed MXene-based anode and $V_2O_5$-PANI cathode in order to create a high voltage window for zinc ion microcapacitor [12]. Huang et al., focused upon the wearable device design and fabrication by involving the use of a flexible zinc ion hybrid capacitor with all-MXenes [13]. A comparison of present work with respect to others is shown in Table S1.

In the present study, a simple and scalable approach was used to fabricate a novel pure MXene-based sensor for pressure sensing, utilizing piezo-resistive and triboelectric concepts. The MXene fabrication was processed using the freeze-dry method, as a superior method compared to conventional approaches. The properties of the fabricated MXene were investigated by several structural and morphological analyses.

## 2. Synthesis methodology

MXene was synthesized using a chemical approach (Fig. 1a). Initially, 50 ml of HCl was mixed with 2 g of LiF and stirred to obtain a homogeneous solution. Small batches of 2 g of MAX phase were gradually added to the solution to avoid splashing. The mixture was continuously stirred for 38 h at 60 °C and centrifuged at 9000 rpm and washed until a neutral pH value. The resulting material was freeze-dried

* Corresponding author.
*E-mail address:* mishra@mci.sdu.dk (Y. Kumar Mishra).

https://doi.org/10.1016/j.matlet.2024.136252
Received 2 January 2024; Received in revised form 22 February 2024; Accepted 3 March 2024
Available online 4 March 2024

to obtain MXene. In the next stage, MXene (300 mg) and DI water (30 ml) solution was prepared (Fig. 1b) and subsequently was bathsonicated for 90 min and followed by centrifugation. Using the vacuum filtration of the supernatant, dry MXene was prepared. In last stage, a rectangular MXene layer (4x2 $cm^2$, thickness ~ 0.1 mm) was inserted between two polydimethylsiloxane (PDMS) layers to avoid oxidation and cured for 10 min at 80 °C [14]. The electrical contacts of the device were made using copper (Cu) wires and silver (Ag) paste. The fabricated device was tested with weight application and finger tapping to obtain a continuous current output and sensitivity. The device was also tested for tribo-electric measurements.

## 3. Experimental techniques

$Ti_3AlC_2$ MAX phase was obtained from Luoyang Tongrun Nano Technology Co, LTD. Lithium fluoride (LiF, 99 %), hydrochloric acid

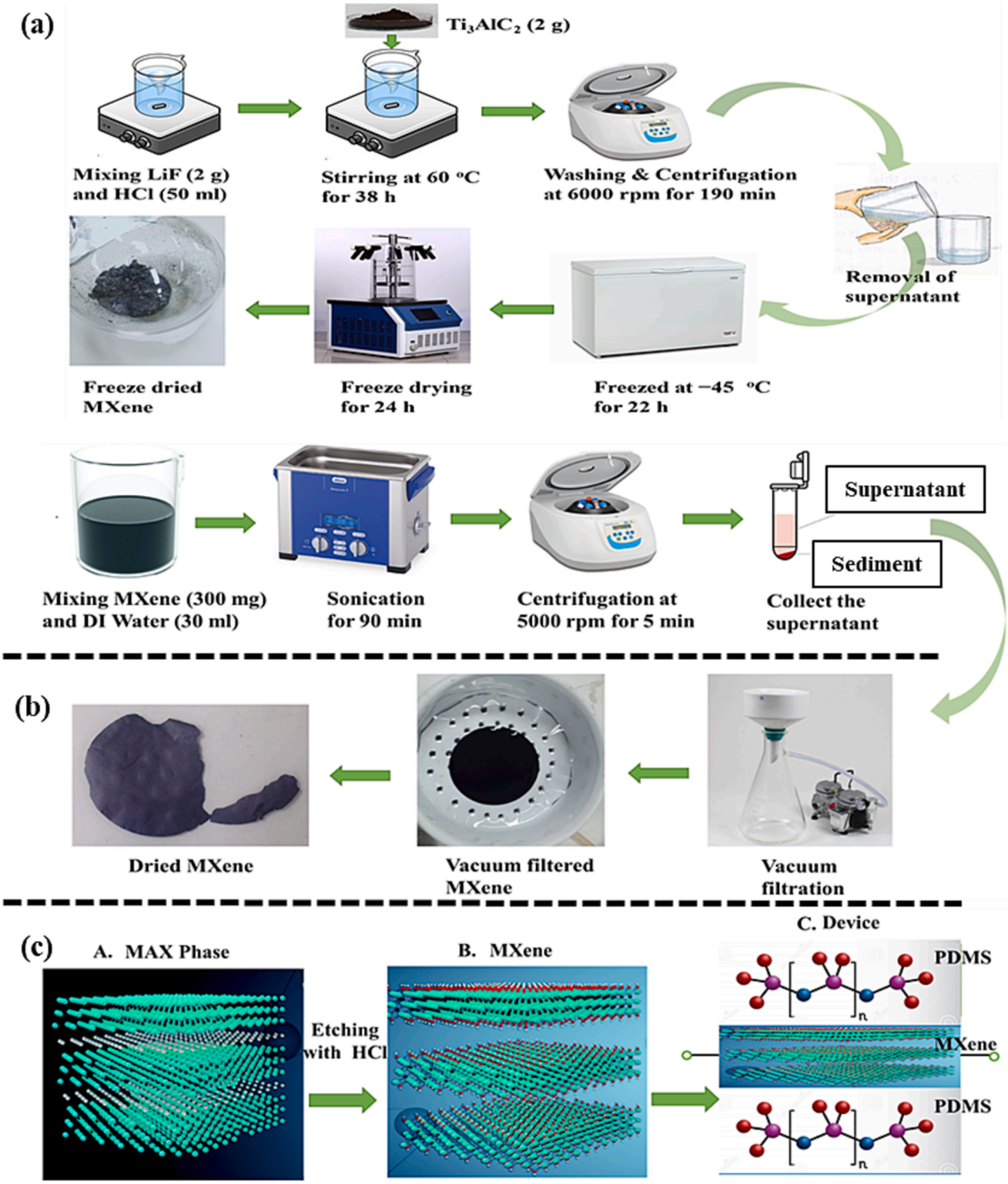


**Fig. 1.** (a) Synthesis process of MXene, (b) Deposition of MXene film and (c) Chemical representation of the material and device.

(HCl, 9 M), PDMS base, and curing agent was obtained by SYLGARD. The synthesized MXene was characterized by a Scanning Electron Microscope (SEM) Hitachi S-4900 and wide-angle XRD (2θ, 5°–80°) for morphological and structural investigations. Raman spectrometer (Renishaw, UK), using 532 nm laser trace Raman spectra. TEM was measured using JEOL JEM 2011. Regulated DC power supply (TPR3003T–3C) and the digital multimeter (DMM6500) were used to obtain electrical measurements. The output of TENG was traced using a Keithley electrometer 6514, USA by utilizing a LabVIEW program interface. The periodic force impact upon the TENG was provided by linear motor (LINMOT, USA).

## 4. Results and discussions

The structural evolution of $Ti_3AlC_2$ shift to $Ti_3C_2T_x$, was successfully validated from XRD spectra with the corresponding 2θ values at 9.58° for the (0 0 2) plane (Fig. 2a). However, the peak shifted from its original position to 6.10°. The second peak at 36.77° corresponds to the (1 0 4) plane of $Ti_3AlC_2$ and this peak has been changed into a broader peak at 36.08° which can be assigned to (1 0 0) plane of MXene. Usually, the crystallographic plane (1 0 4) disappears when the MAX phase is exfoliated to form MXene [14]. The XRD results prove that the Aluminum layers have been selectively etched from the MAX phase [14]. SEM image (Fig. 2b) illustrates a layered structure of MXene [15]. Raman and TEM with elemental color mapping are given in Fig. 2c and d. Current output of piezo-resistive devices (Fig. 3a, b) are obtained for the pressure range of 0.468–0.781 KPa. Multiple measurements were performed to ensure the reproducibility of current output using various weights and mechanical responses were obtained by finger-tapping movement which proved the piezo-resistive effect of MXene. The capability of sensor for monitoring and responding to the mechanical stimulations were obtained from custom-built data acquisition system (Fig. 3c, d). TENG follows the principle of triboelectrification and electrostatic induction for its operation. The digital image and various layers were employed to construct the TENG, and it operated in a vertical contact separation mode (Fig. 4a). The voltage and current response of TENG are shown in Fig. 4(b, c). The long-term stability of TENG device for 1600 s was carried out at constant parameters such as 1 Hz and 5 N (Fig. 4d). The current outputs of TENG at varying frequencies were recorded (Fig. 4e) which was enhanced with frequency increases due to the fast rate of flow of charges through load resistances. Charging of capacitors having various capacities using TENG is presented in Fig. 4f. A bridge rectifier circuit is employed to convert the AC output of TENG to DC signal. The voltage and power outputs of TENG at varying load resistances are shown in Fig. 4(g, h). The highest power of 16 μW at 100 MΩ was recorded for TENG that was utilized as a self-powered weight sensing unit (Fig. 4i). Various weights of 0.06 Kg, 0.08 Kg and 1.72 Kg were placed upon the TENG and removed.

Due to increased mechanical stress, the TENG and pure MXene-based piezo-resistive sensors provided higher output with increased weight, enabling more tribo-electric charge separation. This characteristic is critical for self-powered weight sensing because it allows smart sensing

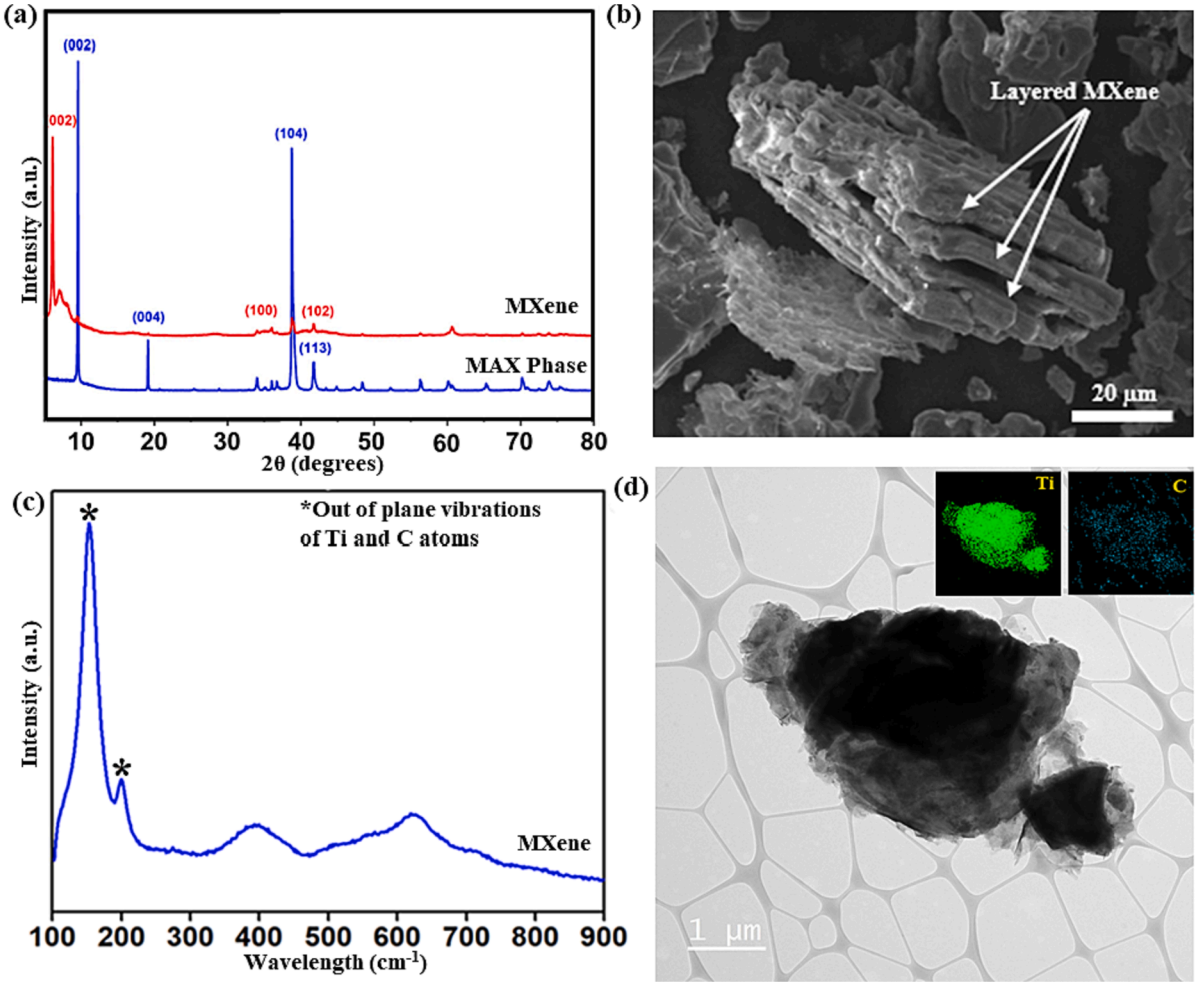


**Fig. 2.** (a) XRD results for the MAX Phase and MXene, (b) Surface morphology of MXene, (c) Raman spectrum for the MXene, and (d) TEM image along with elemental color mapping of synthesized MXene.

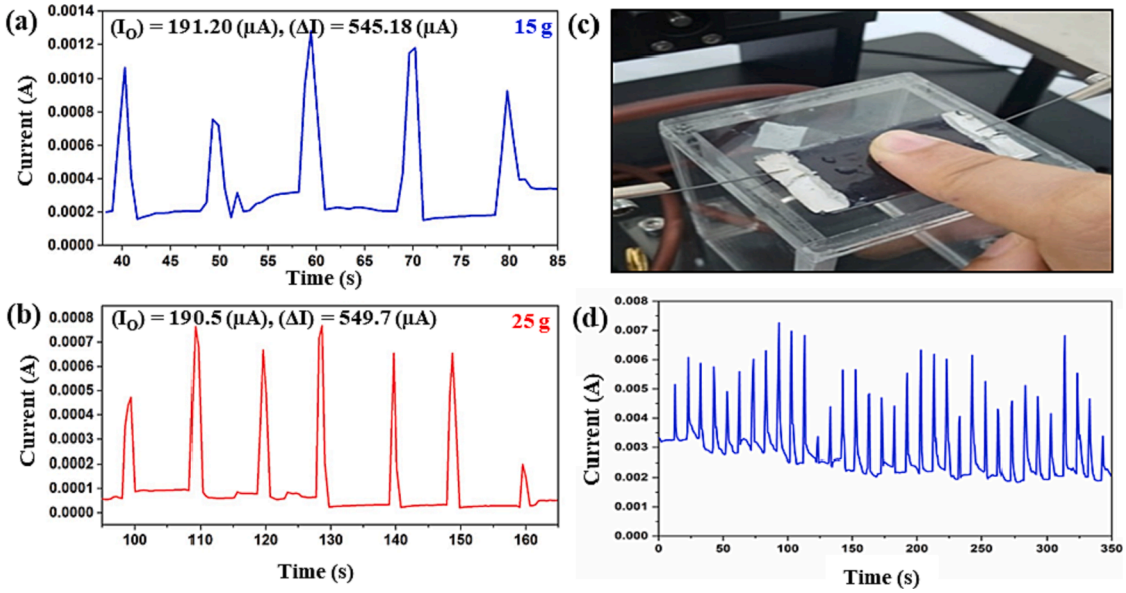


**Fig. 3.** (a) Current vs. time graph for the 0.468 KPa (15 g), (b) 0.781 KPa (25 g), (c) Digital picture of demonstration for the finger tapping and (d) Current Vs. time signals produced by the device for the finger tapping.

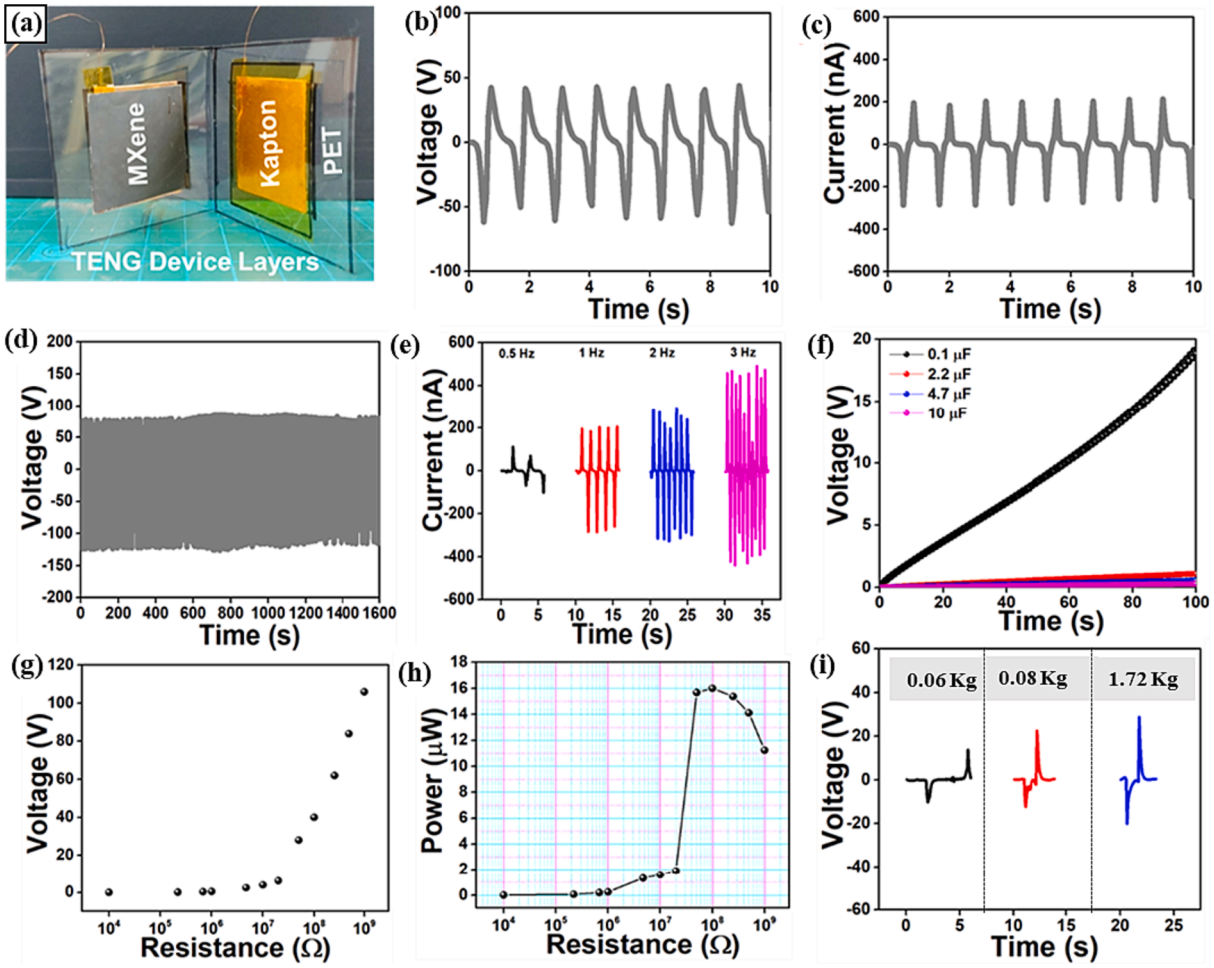


**Fig. 4.** (a) Digital image of device, (b) voltage, (c) current of TENG at 1 Hz and 5N force, (d) Stability of TENG output for 1600 s at 1 Hz and 5N force, (e) Current of TENG at various frequencies, (f) Charging of various capacitors using TENG, (g, h) Voltage and power of TENG at various load resistances and (i) Self-powered weight monitoring using TENG.

and effective energy harvesting from applied force, allowing for sustainable and autonomous operation in weight-sensitive applications compared to MXene-impregnated sensors.

## 5. Conclusions

Pure MXene has been produced by a simple method and has been characterized for structural and morphological characteristics. Experimental findings revealed its high sensitivity to mechanical stimulation, enabling rapid response to pressure changes. The fabricated sensor is appropriate for applications demanding swift detection of pressure or impact, utilizing piezo-resistive and triboelectric energy harvesting. Pure MXene holds promise for energy harvesting, pressure sensors, and self-powered applications.

## CRediT authorship contribution statement

**J.A. Ajani Lakmini Jayarathna:** Writing – review & editing, Writing – original draft, Validation, Resources, Formal analysis, Data curation, Conceptualization. **Sugato Hajra:** Writing – review & editing, Writing – original draft, Formal analysis, Data curation. **Swati Panda:** Writing – review & editing, Writing – original draft, Validation, Formal analysis, Data curation. **Elham Chamanehpour:** Writing – review & editing, Writing – original draft, Visualization, Software, Formal analysis. **Indra Sulania:** Writing – review & editing, Writing – original draft, Visualization, Resources, Formal analysis, Data curation. **Manjeet Singh Goyat:** Writing – review & editing, Writing – original draft, Visualization, Validation, Supervision, Resources, Project administration, Formal analysis, Data curation. **Shu-Han Hsu:** Writing – original draft, Supervision, Resources, Project administration, Funding acquisition, Data curation. **Hoe Joon Kim:** Writing – review & editing, Writing – original draft, Validation, Supervision, Resources, Project administration, Funding acquisition, Formal analysis, Data curation. **Tanyakarn Treeratanaphitak:** Writing – review & editing, Writing – original draft, Supervision, Resources, Funding acquisition, Formal analysis. **Yogendra Kumar Mishra:** Writing – review & editing, Writing – original draft, Validation, Supervision, Resources, Project administration, Methodology, Investigation, Funding acquisition, Formal analysis, Conceptualization.

## Declaration of competing interest

The authors declare no conflict of interest.

## Data availability

Data will be made available on request.

## Acknowledgements

ALJ extend sincere thanks to Sirindhorn International Institute of Technology, Thammasat University for the Faculty's Quota scholarship and Southern Denmark University (SDU) for the support through Erasmus + scholarship. SH, SP, HJK were supported by the Ministry of Trade, Industry and Energy of Korea (RS-2023-00231350). IS and MSG are grateful to the SIRE fellowships (SIR/2022/001573, SIR/2022/001489) awarded from SERB, DST, Govt. of India. SHH and TT acknowledge the support of the Thailand Science Research and Innovation Fundamental Fund through Thammasat University (fiscal year 2024). ALJ, SHH, and TT are partially supported by the Center of Excellence in Functional Advanced Materials Engineering, Thammasat University. YKM thanks the funding from the ESS lighthouse on hard materials in 3D, SOLID (Danish Agency for Science and Higher Education, grant number 8144-00002B), from BHJ Fonden and Fabrikant Mads Clausen Fonden, Denmark.

## Appendix A. Supplementary data

Supplementary data to this article can be found online at https://doi.org/10.1016/j.matlet.2024.136252.

## References

[1] Z. Lou, S. Chen, L. Wang, K. Jiang, G. Shen, Nano Energy 23 (2016) 7–14.
[2] R. Frisenda, E. Navarro-Moratalla, P. Gant, D.P. De Lara, P. Jarillo-Herrero, R. V. Gorbachev, A. Castellanos-Gomez, Chem. Soc. Rev. 47 (2018) 53–68.
[3] J. Tang, X. Huang, T. Qiu, X. Peng, T. Wu, L. Wang, B. Luo, L. Wang, Chem.–A, Eur. J. 27 (2021) 1921–1940.
[4] B. Chen, L. Zhang, H. Li, X. Lai, X. Zeng 617 (2022) 478–488.
[5] H.L. Chia, C.C. Mayorga-Martinez, N. Antonatos, Z.k. Sofer, J.J. Gonzalez-Julian, R. D. Webster, M. Pumera, Anal. Chem. 92 (2020) 2452–2459.
[6] Y. Ma, N. Liu, L. Li, X. Hu, Z. Zou, J. Wang, S. Luo, Y. Gao, Nat. Commun. 8 (2017) 1207.
[7] Y. Guo, M. Zhong, Z. Fang, P. Wan, G. Yu, Nano Lett. 19 (2019) 1143–1150.
[8] Y. Tian, Y. An, B. Xu, Nano Energy (2022) 107556.
[9] Y. Gao, G. Liu, T. Bu, Y. Liu, Y. Qi, Y. Xie, S. Xu, W. Deng, W. Yang, C. Zhang, Nano Res. 14 (2021) 4833–4840.
[10] T. Bhatta, P. Maharjan, H. Cho, C. Park, S.H. Yoon, S. Sharma, M. Salauddin, M. T. Rahman, S.S. Rana, J.Y. Park, Nano Energy 81 (2021) 105670.
[11] S. Zhao, X. Luo, Y. Cheng, Z. Shi, T. Huang, S. Yang, H. Zheng, Y. Bi, J. Zhang, Q. Shi, M. Cao, C. Zhang, Y. Yue, Y. Ma, Chem. Eng. J. 454 (2023) 140360.
[12] A. Li, Z. Wei, Y. Wang, Y. Zhang, M. Wang, H. Zhang, Y. Ma, C. Liu, J. Zou, B. Ge, F. Cheng, Y. Yue, Chem. Eng. J. 457 (2023) 141339.
[13] T. Huang, B. Gao, S. Zhao, H. Zhang, X. Li, X. Luo, M. Cao, C. Zhang, S. Luo, Y. Yue, Y. Ma, Y. Gao, Nano Energy 111 (2023) 108383.
[14] L. Yuan, J. Cai, J. Xu, Z. Yang, H. Liang, Q. Su, J. Wang, Chem. Eng. J. 451 (2023) 139073.
[15] B. Anasori, M.R. Lukatskaya, Y. Gogotsi, Nat. Rev. Mater. 2 (2017) 1–17.